World Academy of Science, Engineering and Technology
International Journal of Mechanical and Mechatronics Engineering
Vol:4, No:12, 2010

Coupling Compensation of 6-DOF Parallel Robot Based on Screw Theory

Ming Cong, Yinghua Wu, Dong Liu, Haiying Wen, Junfa Yu

***Abstract*—**In order to improve control performance and eliminate steady, a coupling compensation for 6-DOF parallel robot is presented. Taking dynamic load Tank Simulator as the research object, this paper analyzes the coupling of 6-DOC parallel robot considering the degree of freedom of the 6-DOF parallel manipulator. The coupling angle and coupling velocity are derived based on inverse kinematics model. It uses the mechanism-model combined method which takes practical moving track that considering the performance of motion controller and motor as its input to make the study. Experimental results show that the coupling compensation improves motion stability as well as accuracy. Besides, it decreases the dither amplitude of dynamic load Tank Simulator.

***Keywords*—**coupling compensation; screw theory; parallel robot; mechanism-model combined motion

I. Introduction

SINCE parallel structure is proposed by D. Stewart [1] in 1965, the 6-DOF parallel robot is one of the most popular cueing simulator mechanisms [2]-[3] for its remarkable advantage over serial mechanisms, where a moving plate is connected to a base plate by six legs. The character of each leg influences the smoothness, accuracy and real-time of the moving plate. This perspective attracts a lot of research on error analysis and compensation.

A. Houssem and H. Bodo opened the discussion on the influence of passive joint friction (PJF) in robot's dynamics and its impact on control performance [4]-[5]. Z. Meng proposed a direct-error-compensation method of measuring the error of a six-freedom-degree parallel mechanism CMM [6]. C. F. Yang developed PD control with gravity compensation for hydraulic 6-DOF parallel manipulator [7]. C. Kevin and A. Tatsuo analyzed the influence of moving plate by the length of each of the six legs [8]. W. Wang studied the coupling characteristics of large hydraulic Stewart Platform [9]. Q. Li compensates the interference of Stewart Platform based on inverse dynamic model [10]. But there are few documents studied on the phenomenon of the coupling. Besides, researchers often use simulation experiment which ignores the performance of motion controller and actuator to make the study [11]-[13]. The experiment results have the deviation with actual value.

In this paper, a coupling compensation is developed to improve the control performance including steady and moving precision via compensating each leg coupling errors. This paper begins with a screw theory to analyze the motion characters of 6-DOF parallel manipulator. Then the Plücker system of leg is built, considering the degree of freedom of the 6-DOF parallel manipulator, and the coupling angle and coupling velocity are calculated by a closed-solution inverse kinematics. Taking dynamic load Tank Simulator as the research object, mechanism-model combined method is described which takes practical moving track as its input to analyze the performance including stability and precision of the moving plate.

Ming Cong, Yinghua, Wu, Dong Liu, Haiying Wen are with the School of Mechanical Engineering, Dalian University of Technology, Dalian, China (e-mail: wuyinghuagirl@163.com).

Junfa Yu is with the NO.65053 Army, Dalian, China (e-mail: alf833@163.com).

II. Coupling Analysis and Compensation by Screw Theory

A. Coupling Analysis

With reference to Fig. 1, which represents the 6-DOF parallel robot structure here considered, it can be observed that the moving plate and the base plate are combined with six legs which consist of upper gimbal, screw joint and lower gimbal. One of the combined legs is taken to analyze its coupling based on screw theory.

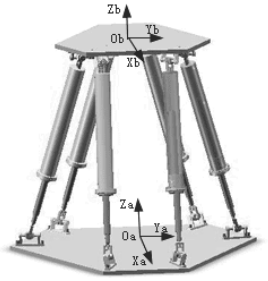

Fig.1 Model of 6-DOF parallel robot

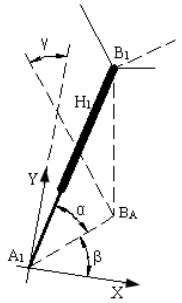

Fig. 2 Coordinate system of leg $A_1H_1B_1$

It supposes that the coupling does not exist in each screw

joint of legs, which means the screw joint, as same as translational joint, has only one translational motion. The frame (X, Y, Z) located at the center of the lower gimbal is shown in Fig.2.The lower gimbal A1 contains two orthogonal rotational motion which are given in Plücker coordinates by:

$$\$_1 = [1\ 0\ 0\ ;\ 0\ 0\ 0] \tag{1}$$

$$\$_2 = [0\ 1\ 0\ ;\ 0\ 0\ 0] \tag{2}$$

The angle between the line of translational motion and the base plate is denoted by α, the angle between the X-axis and the line of A_1B_A which is the projection of A_1B_1 is denoted by β. Thus, the translational motion of screw joint is given in Plücker coordinates by:

$$\$_3 = [0\ 0\ 0\ ;\ \cos\alpha\cos\beta \quad \cos\alpha\sin\beta \quad \sin\alpha] \tag{3}$$

The upper gimbal also contains two orthogonal rotational motions. Length of the leg A_1B_1 is denoted by L_1, γ stands for the angle between the line of the upper gimbal center joint and the opposing lower gimbal center joint. Thus, the two orthogonal rotational motion of the upper gimbal can be calculated in Plücker coordinates as follows:

$$\$_4^1 = [-\sin\gamma\ \ \cos\gamma\ \ 0] \tag{4}$$

$$\begin{aligned}\$_4^0 &= r \times \$_4^1 = OB_1 \times \$_4^1 \\ &= [-l\sin\alpha\cos\gamma \quad -l\sin\alpha\sin\gamma \\ &\quad l\cos\alpha\cos\beta\cos\gamma + l\cos\alpha\sin\beta\sin\gamma]\end{aligned} \tag{5}$$

$$\$_4 = [\$_4^1\ ;\ \$_4^0] \tag{6}$$

$$\begin{aligned}\$_5^1 &= \$_4^1 \times \frac{r}{|r|} = [\sin\alpha\cos\gamma \quad \sin\alpha\sin\gamma \\ &\quad -\cos\alpha\sin\beta\sin\gamma - \cos\alpha\cos\beta\cos\gamma]\end{aligned} \tag{7}$$

$$\begin{aligned}\$_5^0 &= r \times \$_5^1 = OB_1 \times \$_5^1 \\ &= [-l\cdot\cos^2\alpha\cdot\sin^2\beta\cdot\sin\gamma - l\cdot\cos^2\alpha\cdot\sin\beta\cdot \\ &\quad \cos\beta\cdot\cos\gamma - l\cdot\sin^2\alpha\cdot\sin\gamma \quad l\cdot\sin^2\alpha\cdot \\ &\quad \cos\gamma + l\cdot\cos^2\alpha\cdot\sin\beta\cdot\cos\beta\cdot\sin\gamma + l\cdot \\ &\quad \cos^2\alpha\cdot\cos^2\beta\cdot\cos\gamma \quad l\cdot\sin\alpha\cdot\cos\alpha\cdot\cos\beta\cdot \\ &\quad \sin\gamma - l\sin\alpha\cos\alpha\sin\beta\cos\gamma]\end{aligned} \tag{8}$$

$$\$_5 = [\$_5^1\ ;\ \$_5^0] \tag{9}$$

Therefore, the screw system of leg $A_1H_1B_1$ is given as:

$$\$_{A_1H_1B_1} = \begin{bmatrix}\$_1\\ \$_2\\ \$_3\\ \$_4\\ \$_5\end{bmatrix} \tag{10}$$

Thus the anti-screw system of leg $A_1H_1B_1$ has 1 DOF which is denoted by:

$$\$^r_{A_1H_1B} = [L\ \ M\ \ N\ \ P\ \ Q\ \ R] \tag{11}$$

where P=0, Q=0. L, M, N can be expressed by R.

In the same manner, each of the leg has one constraint motion, the degrees of freedom of the moving plate is no more than 6. The result does not match with actual situation. While the anti-screw system of leg $A_1H_1B_1$ has a rotational motion along the line of A_1B_1 when R=0. It supposes that coupling exits in legs moving, the constraint of leg is released. Thus the moving plate has three translational motions and three rotational motions. Therefore, the coupling exits in each leg indeed.

B. Coupling Compensation

There are two frames describing the motion of the moving plate: an inertia frame (X_a, Y_a, Z_a) located at the center of the base plate and a body frame (X_b, Y_b, Z_b) located at the center of the moving plate with Z_b-axis pointing outward (Fig.1). The length vector of the ith leg is calculated as:

$$L_i^A = B_i^A - A_i^A\ ,\ i=1\ ,\ \ldots\ ,\ 6 \tag{12}$$

where A_i^A is the position of the lower joint A_i in the inertia frame, B_i^A is the position of the upper joint B_i in the inertia frame.

$$B_i^A = {}^AT_B \cdot B_i^B \tag{13}$$

where ${}^AT_B$ is the transformation matrix form the body frame (X_b, Y_b, Z_b) to the inertia frame (X_a, Y_a, Z_a), B_i^B is the position of the upper joint B_i in the plate body frame.

The leg can rotate around the axis of gimbal, while the upper part of the leg is sliding inside the lower part by an actuating force. This motion is considered by two frames: a leg fixed frame (X_{ni}, Y_{ni}, Z_{ni}) located at the joint A_i with the Z_{ni}-axis parallel to the length vector of leg and X_{ni}-axis parallel to the rotational axis of lower gimbal in outward, the leg body frame (X_{mi}, Y_{mi}, Z_{mi}) located at the same point with X_{mi}-axis parallel to the rotational axis of upper gimbal as shown in Fig.3.

Fig.3 One Leg of the 6-DOF parallel robot

$$Z_{mi} = \frac{L_i^A}{\left|L_i^A\right|} \tag{14}$$

$$X_{mi} = \frac{Z_{mi} \times G_{mi}^A}{\left|Z_{mi} \times G_{mi}^A\right|} \tag{15}$$

where G_{mi}^A is the installation vector of the upper gimbal in the inertia frame, $G_{mi}^A = {}^A T_B G_{mi}^B$, G_{mi}^B is the installation vector of the upper gimbal in the plate body frame.

$$Z_{ni} = Z_{mi} \tag{16}$$

$$X_{ni} = \frac{Z_{ni} \times G_{ni}^A}{\left|Z_{ni} \times G_{ni}^A\right|} \tag{17}$$

where G_{ni}^A is the installation vector of the lower gimbal in the inertia frame.

There are 2 DOF between the leg fixed frame (X_{ni}, Y_{ni}, Z_{ni}) and the leg body frame (X_{mi}, Y_{mi}, Z_{mi}): one translational motion alone Z_{ni}-axis and one rotational motion around Z_{ni}-axis. The coupling angle ψ_i is then calculated as:

$$\left|\psi_i\right| = \arccos \frac{X_{mi} \cdot X_{ni}}{\left|X_{mi}\right|\left|X_{ni}\right|} \tag{18}$$

where ψ_i is positive number when $X_{mi} \times X_{ni}$ have the same direction with L_i^A, otherwise ψ_i is negative number.

The angular velocity ω_{si} of coupling is given as:

$$\omega_{si} = \dot{\psi}_i = \frac{M}{\left|X_{mi}\right|\left|X_{ni}\right|\sqrt{1+\left(\frac{X_{mi} \cdot X_{ni}}{\left|X_{mi}\right|\left|X_{ni}\right|}\right)^2}} \tag{19}$$

where

$$M = \frac{\left(\frac{v_{bi}}{\left|L_i^A\right|} \times G_{mi}^A + Z_{mi} \times JG_{mi}^B\right) X_{ni}}{\left|Z_{mi} \times G_{mi}^A\right|} + \frac{\frac{X_{mi}}{\left|L_i^A\right|}\left(v_{bi} \times G_{ni}^A\right)}{\left|Z_{ni} \times G_{ni}^A\right|}$$

, J is the Jacobian matrix of the general velocity of the moving plate to the velocity of the upper attachment points.

The difference of the *i*th leg between practice and theory Δ_i is computed as:

$$\Delta_i = \frac{\psi_i}{2\pi} \cdot Da \tag{20}$$

where Da is the screw-pitch.

Therefore, the practical length of the *i*th L_t is given as:

$$L_{ti} = l_i + \left(\Delta_i - \Delta_{pi}\right) \tag{21}$$

where Δ_{pi} is the difference of the *i*th leg between practice and theory in the previous moving plate position.

III. Experiment of Mechanism-Model Combined Motion

A. Experimental Methods Compared

This paper investigates two methods (mechanism-model combined motion method and theory method) to test the precision of the motion. Taking the sine curve of the moving plate rotated around Z_a-axis as the research process, the controlling pulse curve of 1th and 2th 6-DOF parallel robot leg are extracted without coupling compensation as shown in Fig.4.

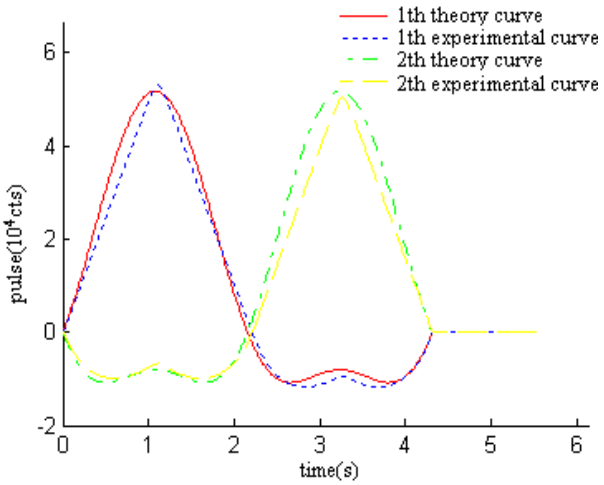

Fig.4 Theory pulse curve and experimental pulse curve without coupling compensation

The theory method neglects two main aspects as follows which may cause the difference between theory pulse curve and experimental pulse curve.

1) The influence of motion controller. Theory pulse curve does not consider the influence of the motion controller to the data sending and receiving speed as well as operating speed.
2) The influence of actuator. Some characteristics of actuator are variable. They are changing with the motion of actuator. While the theory method does not contains the variable quantity that may cause the difference.

Taking the experimental pulse curves as input, the mechanism-model combined motion method improves the precision and authenticity of the 6-DOF parallel robot model. Besides, it is beneficial to research on the own characters of 6-DOF parallel robot.

B. Extracting Actuator Speed

This paper takes Tank Simulator which base on 6-DOF parallel robot as research object (Fig.5). Each leg has an upper part sliding inside a lower part to imitate the physical feeling of driving a Tank for the three translational motions (surge, sway, and heave) and the three rotational motions (pitch, roll, and yaw). The proposed scheme applied to the Tank Simulator is given in TABLE I.

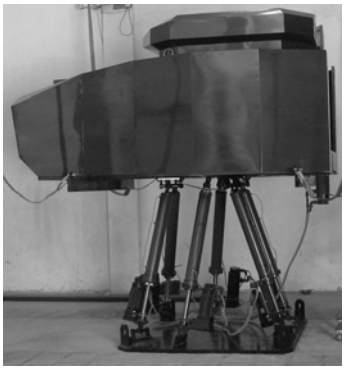

Fig.5 Photo of Tank Simulator test prototype

TABLE I
PARAMETERS OF THE TANK SIMULATOR

Symbol	Description	Value
Rb(m)	Radius of the movable plate	0.4
Ra(m)	Radius of base plate	0.8
β(°)	Joint angles of upper plate	[40, 80, 160, 200, 280, 320]
α (°)	Joint angles of base plate	[20, 100, 140, 220, 260, 340]
H(m)	Center height of Tank Simulator	1.4
m(t)	Payload of Tank Simulator	2

The principle diagram of mechanism-model combined motion method is shown in Fig.6. Feedback curves of Tank Simulator actuator are extracted. Then taking these curves as input of 6-DOF parallel robot model, the moving plate of model has the same motion with Tank Simulator. The velocity feedback of 1th and 2th leg of Tank Simulator is shown in Fig.7.

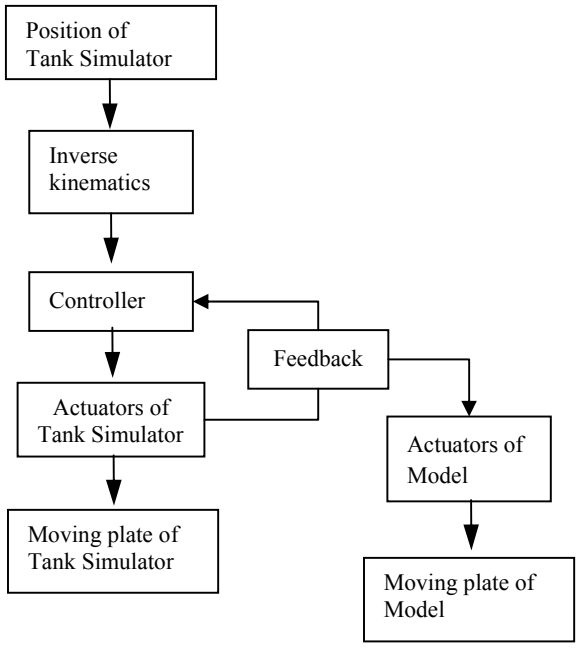

Fig.6 Mechanism-model combined experiment schematic diagram

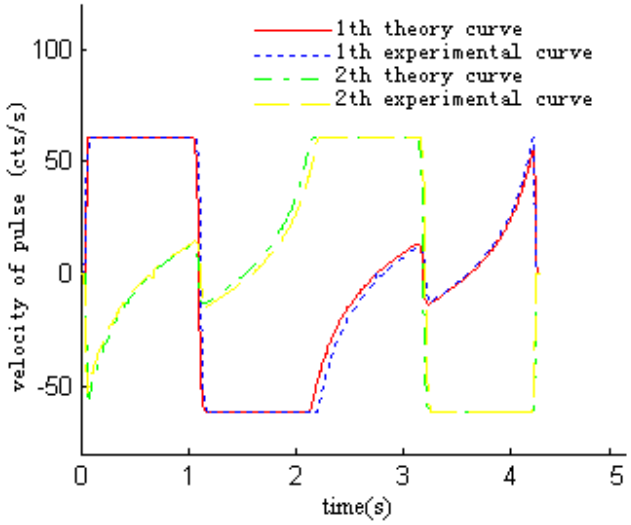

Fig.7 Experimental curves of velocity feedback

IV. EXPERIMENT RESULTS

Tank Simulator rotated around Z_a-axis to make the sinusoidal motion which amplitude is 30°. Taking the velocity as the input of 6-DOF parallel robot model, this paper analyzes performance of Tank Simulator. The experimental results of errors are shown in the TABLE II. Without the coupling compensation, 6-DOF parallel robot generates an error on the direction of Z-axis. Rotated angle and translational distance of Z-axis is shown in Fig.8 and Fig.9. Besides, Fig.10 and Fig.11 show the translational velocity and acceleration of Z-axis.

TABLE II
ERROR OF THE 6-DOF PARALLEL ROBOT

	Z/°	Y/°	X/°	z/mm	y/mm	x/mm
Theoretical export	30sin(t)	0	0	0	0	0
Error without compensation	0.36	0	0	1.74 sin(t)	0	0
Error with compensation	0.19	0	0	0.21	0	0

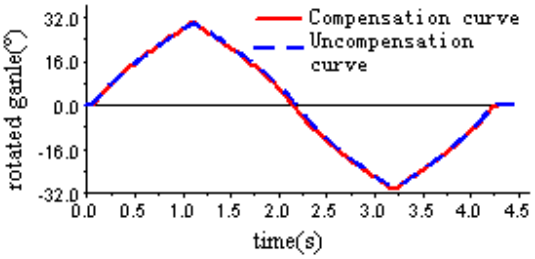

Fig.8 Rotational angle on Z axis

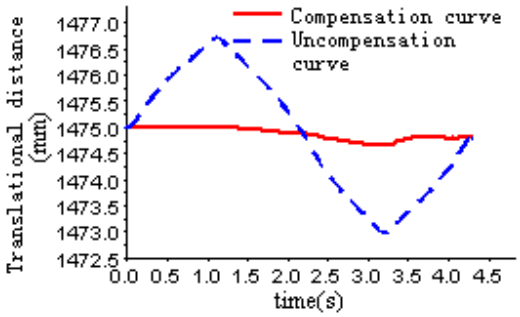

Fig.9 Movement distance on Z axis

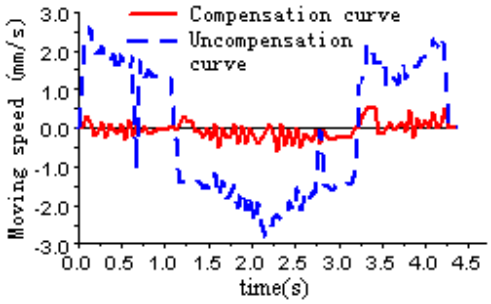

Fig.10 Moving speed of Z axis

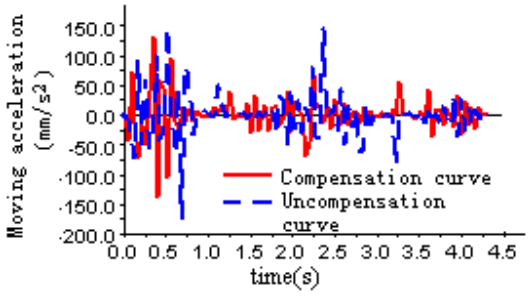

Fig.11 Moving acceleration of Z axis

From the experiment results, it is obvious that the motion on command direction according to preconceived track with accurate amplitude and period, but the error on translation along with Z-axis is big which can causes vibration of Tank Simulator that can not neglect. All coordinate values, especially the Z coordinate value, decreased dramatically after the coupling compensation of 6-DOF parallel robot. The variation of moving velocity on Z-axis after the compensation was decreased 82%, acceleration has decreased from 175mm/s^2 to 140 mm/s^2. In the same manner, taking the rotation of X-axis or Y-axis as the research process, the translational error on X-axis or Y-axis decreased dramatically. As the maximum velocity is limited by controller, exercise time is prolonged. Movement distance on X-axis and Y-axis are shown as Fig.13 and Fig.14.

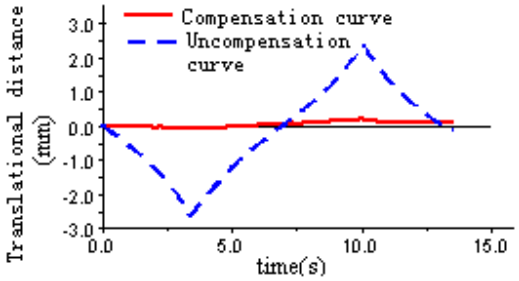

Fig.12 Movement distance on X axis

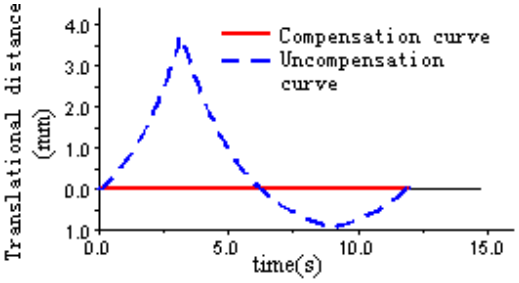

Fig.13 Movement distance on Y axis

V. CONCLUSION

In this paper, the motion of 6-DOF parallel robot is studied base on screw theory. The following conclusions can be drawn:

1) Due to analysis of the legs of 6-DOF parallel robot model, there exists coupling between the six degrees of freedom. In this paper, it builds the coupling velocity and acceleration. Besides, the coupling compensation is proposed to optimize the moving track.
2) Mechanism-model combined motion method which is presented in this paper considers the influence of the motion controller and actuator that can improves the reliability and authenticity of 6-DOF parallel robot.
3) Experimental results show that the precision can be increased by the coupling compensation. It eliminates jitter in the motion that can prolong life of Tank Simulator.

REFERENCES

[1] D. Stewart, "A platform with six degrees of freedom," in *Proceeding of Institute of Mechanical Engineering*, London, 1965, pp. 371-386.

[2] Q. T. Huang, H. Z. Jiang, S. Y. Zhang, "Spacecraft docking simulation using hardware-in-the-loop simulator with Stewart platform," *Journal of Mechanical Engineering*, vol 18, no. 3, pp. 415-418, Sep. 2005.
[3] H. Q. Yang, K. D. Zhao, S. L. Wu, J. Cao, "Key technologies and developing state of 6-DOF motion system for Flight Simulator," *Journal of System Simulation*, vol 14, no. 1, pp. 84-87, Jan. 2002.
[4] H. Abdellatif, B. Heimann, "On compensation of passive joint friction in robotic manipulators: modeling, detection and identification," in *Proceedings of the IEEE International Conference on Control Applications,* Munich, 2006, pp. 2510-2515.
[5] H. Abdellatif, M. Grotjahn, B. Heimann, "Independent identification of friction characteristics for parallel manipulators", *Journal of Dynamic Systems, Measurement and Control, Transactions of the ASME*, vol 129, no. 3, pp. 294-302, May 2007.
[6] Z. Meng, R. S. Che, Q. C. Huang, Z. J. Yu, "The direct-error-compensation method of measuring the error of a six-freedom-degree parallel mechanism CMM," *Journal of Materials Processing Technology*, vol 129, no.1-3, pp. 574-578, Oct.2002.
[7] C. F. Yang, Q. T. Huang, H. Z. Jiang, P. O. Ogbobe, J. W. Han, " PD control with gravity compensation for hydraulic 6-DOF parallel manipulator," *Mechanism and Machine Theory*, vol 45, no. 4, pp. 666-677, Apr. 2010.
[8] C. Kevin, A. Tatsuo, "A prototype parallel manipulator: kinematics, construction, software, workspace results, and singularity analysis," *Proceedings-IEEE International Conference on Robotics and Automation*, Sacramento, 1991, pp. 566-571.
[9] W. Wang, H. B. Xie, X. Fu, H. Y. Yang, "Coupling characteristics of large hydraulic Stewart Platform," *Journal of Mechanical Engineering*, vol 43, no. 9, pp. 12-15, Sep. 2007.
[10] Q. Li, X. Y. Wang, J. Cheng, "Interference force compensation of Stewart Platform based on inverse dynamic model," *Journal of Mechanical Engineering*, vol 45, no.1, pp. 14-19, Jan. 2009.
[11] J. M. Ma, J. F. He, H. G. Xiong, J. W. Han, "Simulation of coupling characteristic of hydraulically driven Stewart Platform based On dynamics model," *Proceedings-2008 International Workshop on Modeling, Simulation and Optimization, WMSO 2008*, pp. 88-92, 2009, *Proceedings – 2008 International Workshop on Modeling, Simulation and Optimization, WMSO 2008*.
[12] S. Iqbal, A. I. Bhatti, Q. Ahmed, "Determination of realistic uncertainty bounds for the Stewart Platform with payload dynamics," *Proceedings of the IEEE International Conference on Control Applications*, pp. 995-1000,2008, *17th IEEE International Conference on Control Applications, CCA*.
[13] S. Liu, W. L. Li, Y. C. Du, J. Song, "Dynamic simulation of submarine Stewart platform," *Journal of Harbin Institute of Technology*, vol 41, no.9, pp. 249-255, Sep. 2009.